analytical chemistry

pubs.acs.org/ac Article

Electrochemically Controlled ATRP for Cleavage-Based Electrochemical Detection of the Prostate-Specific Antigen at Femtomolar Level Concentrations

Qiong Hu, Shiyu Gan, Yu Bao, Yuwei Zhang,* Dongxue Han, and Li Niu

Cite This: https://dx.doi.org/10.1021/acs.analchem.0c03467 Read Online

ACCESS | Metrics & More | Article Recommendations | Supporting Information

ABSTRACT: As a single-chain glycoprotein with endopeptidase activity, the prostate-specific antigen (PSA) is valuable as an informative serum marker in diagnosing, staging, and prognosis of prostate cancer. In this report, an electrochemical biosensor based on the target-induced cleavage of a specific peptide substrate (PSA peptide) is designed for the highly selective detection of PSA at the femtomolar level, using electrochemically controlled atom transfer radical polymerization (eATRP) as a method for signal amplification. The PSA peptides, without free carboxyl sites, are attached to the gold surface via the *N*-terminal cysteine residue. The target-induced cleavage of PSA peptides results in the generation of carboxyl sites, to which the alkyl halide initiator α-bromophenylacetic acid (BPAA) is linked via the Zr(IV) linkers. Subsequently, the potentiostatic eATRP of ferrocenylmethyl methacrylate (FcMMA, as the monomer) leads to the surface-initiated grafting of high-density ferrocenyl polymers. As a result, a large amount of Fc redox tags can be recruited for signal amplification, through which the limit of detection (LOD) for PSA can be down to 3.2 fM. As the recognition element, the PSA peptide is easy to synthesize, chemically and thermally stable, and low-cost. Without the necessity of enzyme or nanoparticle labels, the eATRP-based amplification method is easy to operate and low-cost. Results also show that the cleavage-based electrochemical PSA biosensor is highly selective and applicable to PSA detection in complex biological samples. In view of these merits, the integration of the eATRP-based amplification method into cleavage-based recognition is believed to hold great promise for the electrochemical detection of PSA in clinical applications.

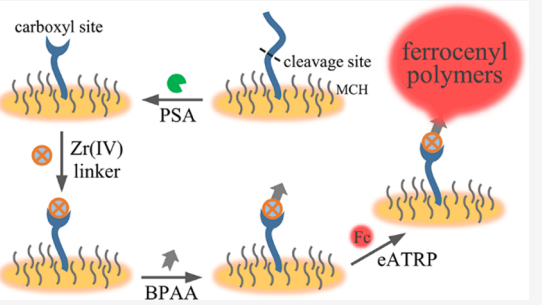

Since the mid-1980s, prostate cancer has become the second leading cause of cancer death in men in the United States, and the number of death cases in 2020 is estimated to be 33 330.[1] The diagnosis, staging, and prognosis of prostate cancer based on the clinical screening of various serum markers, such as prostatic acid phosphatase (PAP), thymidine kinase (TK), prostate-specific membrane antigen (PSMA), and prostate-specific antigen (PSA), has attracted much attention due to the low invasiveness of liquid biopsy.[2] PSA, also called kallikrein-3 (KLK3), is a single-chain glycoprotein encoded by the *KLK*3 gene. It is a serine protease with chymotrypsin-like endopeptidase activity. As one of the highly abundant proteases in the seminal fluid, its function is to cleave semenogelins, and thus it is responsible for the liquefaction of the seminal coagulum. PSA is secreted almost exclusively by the epithelial cells of the prostate gland, and high tissue specificity makes it valuable as a promising serum marker for prostate cancer, with a threshold value of 4 ng mL^{-1} for clinical screening.[3] Clearly, the detection of PSA is of great value in clinical applications.

In addition to the fluorescence,[4,5] colorimetric,[6,7] light scattering-based,[8,9] electrochemiluminescence (ECL),[10,11] chemiluminescence (CL),[12] electrical,[13,14] photoelectrochemical (PEC),[15−17] surface-enhanced Raman scattering (SERS),[18,19] quartz crystal microbalance (QCM),[20] and surface plasmon resonance (SPR)-based methods,[21] a series of electrochemical biosensors have been designed for PSA detection,[22−25] in view of their merits such as good portability, high selectivity and sensitivity, and fast response. For electrochemical PSA biosensors, the selectivity can be sufficiently high when using molecularly imprinted polymers (MIPs),[26] nucleic acid aptamers,[27] anti-PSA antibodies,[28−32] and peptide substrates[33−35] as the molecular recognition elements (MREs). For affinity recognition by MIPs, aptamers, or antibodies, PSAs are captured by the binding sites in an equimolar ratio; for the cleavage-based recognition by peptide substrates, on the other hand, the presence of a PSA can result in the enzymatic cleavage of hundreds to thousands of peptide fragments. As a result, the detection sensitivity through

Received: August 14, 2020
Accepted: November 2, 2020

https://dx.doi.org/10.1021/acs.analchem.0c03467
Anal. Chem. XXXX, XXX, XXX−XXX

cleavage-based recognition is inherently much higher than that through affinity recognition. Besides, the cleavage-based recognition is specific to the detection of the clinically relevant form of PSA (i.e., the active PSA with enzymatic activity), which is impossible for affinity recognition. Since the landmark work of Roberts and Kelley in 2007,[34] the cleavage-based recognition has attracted considerable attention in the electrochemical detection of PSA. Using the ferrocene-tagged peptide substrate as the MRE, for example, Zhao et al. designed an electrochemical PSA biosensor, in which the target-induced cleavage of peptide substrates correlated with the loss of ferrocene (Fc) redox tags.[33] Although it is easy to operate and sufficient for clinical screening, the limit of detection (LOD) of 0.2 ng mL^{-1} is not very impressive. This is due to the fact that in such design, one cleavage event could result in the loss of only a redox tag. To further down-regulate the LOD of the cleavage-based electrochemical PSA biosensors, the gold nanoparticles (AuNPs)-induced silver enhancement has been exploited for signal amplification, through which the LOD of PSA can be down to 0.7 pg mL^{-1}.[35] Nevertheless, the preparation of the DSP@Au@SiO_2 nanocomposites (DSP, dithiobis(succinimidyl propionate)) is quite a cumbersome and time-consuming task, which hampers its potential use. As we know, sensitivity, selectivity, and simplicity are three of the most critical criteria for evaluating the practicability of a biosensor. As selectivity is determined by peptide substrates, the practicability of the cleavage-based electrochemical PSA biosensors can only be substantially improved when an easy to operate method is applied for signal amplification, considering that in such a case, both the sensitivity and simplicity can be simultaneously improved.

Since the pioneering work of He and co-workers in 2005,[36] atom transfer radical polymerization (ATRP), as a robust method for signal amplification, has attracted growing attention for the detection of biomolecules of clinical relevance,[37−40] such as proteins[41−43] and nucleic acids.[44−46] For example, the activator generated by electron transfer for ATRP (AGET ATRP) was applied for the visual detection of ovalbumin and insulin;[42] through the AGET ATRP of 2-hydroxyethyl methacrylate (HEMA), the formation of the poly(HEMA) spots on a highly reflective substrate would result in a change of surface opacity, which can be visualized by the naked eye. Using electrochemically controlled ATRP (eATRP) as a method for signal amplification, a peptide nucleic acid (PNA)-based electrochemical biosensor has been designed for the highly sensitive and selective detection of DNA fragments.[45] As a powerful reversible-deactivation radical polymerization (RDRP), ATRP relies on the use of alkyl halides (R−X, X = Cl, Br) as the initiators, Cu^{I}/ligand complexes as the activators, and the corresponding $Cu^{II}X$/ligand complexes as the deactivators.[47,48] Because there are a wide variety of ATRP initiators, ligands (e.g., tris[2-(dimethylamino)ethyl]amine (Me_6TREN)), and vinyl monomers (e.g., (meth)acrylamides and (meth)acrylates) commercially available for use, ATRP is a versatile method for signal amplification. Typically, the ATRP-based method is operated through (i) the labeling of alkyl halide initiators and (ii) the ATRP-mediated surface-initiated grafting of polymers; clearly, it is not only easy to operate but also low-cost. As a result, ATRP shows great promise as a method for signal amplification.

Inspired by these merits, herein, we illustrate a novel cleavage-based electrochemical biosensor for the highly selective detection of PSA at the femtomolar level, using eATRP as a method for signal amplification. The principle of the cleavage-based electrochemical PSA biosensor is shown in Scheme 1. For the recognition of PSA, the peptide substrate

Scheme 1. Schematic Illustration of the Cleavage-Based Electrochemical PSA Biosensor

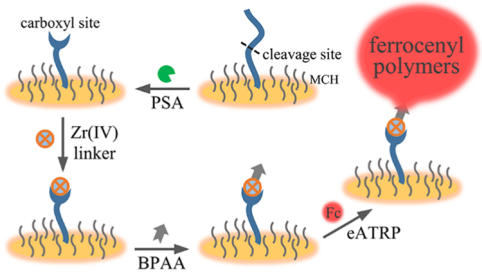

CSGGSSHSSKLQKK-$CONH_2$ that can be cleaved by PSA at the carboxyl side of the glutamine residue is end-attached to a gold surface via the *N*-terminal cysteine residue. The hexapeptide HSSKLQ is the specific recognition site for PSA, with the Michaelis constant (K_m) of 470 μM.[49] After the target-induced cleavage of peptide substrates, the alkyl halide initiators α-bromophenylacetic acid (BPAA) are linked to the cleaved sites via the well-established carboxylate-Zr(IV)-carboxylate linkage. Using ferrocenylmethyl methacrylate (FcMMA) as the vinyl monomer, the surface-initiated grafting of the poly(FcMMA) polymers through eATRP brings a large amount of Fc redox tags onto the electrode surface, generating a significantly amplified detection signal. Specifically, the eATRP-mediated grafting is operated through the potentiostatic reduction of the $Cu^{II}Br/Me_6$TREN deactivators into the Cu^{I}/Me_6TREN activators, which react with the BPAA initiators to form the initiating radicals ($R^{\bullet}$) that are capable of continuous FcMMA monomer addition to form the propagating radicals ($P_n^{\bullet}$) and eventually the ferrocenyl polymers.[45] The results demonstrated that the integration of the eATRP-based method into cleavage-based recognition is applicable for the highly selective detection of PSA at the femtomolar level (LOD, 3.2 fM). Also, the cleavage-based biosensor shows great promise for the electrochemical detection of PSA in complex biological samples.

EXPERIMENTAL SECTION

Materials and Reagents. PSA peptide CSGGSSHSSKLQKK-$CONH_2$ with purity higher than 95% was supplied by Shanghai Science Peptide Biological Technology Co., Ltd. (Shanghai, China). PSA from human seminal fluid (molecular weight, 34 kDa; buffered aqueous solution), carcinoembryonic antigen (CEA) from human colon cancer (buffered aqueous solution), α-fetoprotein (AFP) from human fetal cord serum (buffered aqueous solution), and bovine immunoglobulin G (IgG) were offered by Shanghai Linc-Bio Science Co., Ltd. (Shanghai, China). Chymotrypsin (chymo) and trypsin (tryp) from porcine pancreas were collected from Sangon Biotech (Shanghai) Co., Ltd. (Shanghai, China). Lithium perchlorate trihydrate ($LiClO_4$), normal human serum (NHS), and FcMMA were supplied by Aladdin Bio-Chem Technology Co., Ltd. (Shanghai, China), Shanghai YiJi Industries Co., Ltd. (Shanghai, China), and Shanghai Pharmlead Inc (Shanghai, China), respectively. Human hemoglobin (Hb), 6-mercapto-1-hexanol (MCH),

https://dx.doi.org/10.1021/acs.analchem.0c03467
Anal. Chem. XXXX, XXX, XXX−XXX

and zirconium dichloride oxide octahydrate ($ZrOCl_2$) were from Sigma-Aldrich. Anhydrous $CuBr_2$, Me_6TREN, $K_3Fe(CN)_6$, KPF_6, $K_4Fe(CN)_6$, albumin from bovine serum (BSA), and BPAA were offered by J&K Scientific Ltd. (Shanghai, China). Anhydrous ethanol and others were from Sinopharm Chemical Reagent Co., Ltd. (Shanghai, China). All chemicals, analytical grade or higher, were used directly. Ultrapure water (≥18.25 MΩ cm, ddH_2O) used in this study was from a Millipore Milli-Q purification system.

The stocking and washing buffer for PSA was 10 mM Na_2HPO_4/NaH_2PO_4 (PBS, containing 0.15 M NaCl, pH 7.4). The solution for electrochemical impedance spectroscopy (EIS) measurements was 5 mM $Fe(CN)_6^{3-/4-}$ in 0.1 M KNO_3. The polymerization solution was prepared by adding 100 μL of 10 mM FcMMA in *N*,*N*-dimethylformamide (DMF), 100 μL of 10 mM $Cu^{II}Br/Me_6TREN$ in DMF, 1 mL of 1 M KBr, and 6 mL of 0.1 M KPF_6 to 2.8 mL of DMF. Piranha solution is a 3:1 (v/v) mixture of 98% H_2SO_4 and 30% H_2O_2 and should be freshly prepared for each use and handled with great care.

Apparatus. EIS (initial frequency, 100 kHz; final frequency, 0.1 Hz; potential amplitude, 5 mV) was measured, at the open circuit potential, using a Reference 600+ potentiostat/galvanostat (Gamry Instruments). Other electrochemical measurements were carried out with a CHI760E electrochemical workstation (CH Instruments). Electrochemical measurements were performed at room temperature with a routine three-electrode setup: working electrode, the modified polycrystalline gold electrode (AuE, 3 mm in diameter); reference electrode, a saturated calomel electrode (SCE); and counter electrode, a platinum wire. The surface morphology of the as-modified AuE was studied at an accelerating voltage of 15 kV with a field emission scanning electron microscope (FE-SEM, JSM-7100F, JEOL).

Cleavage-Based Electrochemical Detection of PSA. Prior to use, AuE was polished carefully with 0.3 μm γ-Al_2O_3 slurry, cleaned by sequential sonication in ethanol and ddH_2O, soaked in fresh piranha solution at 80 °C for 0.5 h, rinsed with ddH_2O, scanned at 0.1 V s^{-1} by cyclic voltammetry (CV, cycling between −0.3 and 1.5 V) in 0.5 M H_2SO_4 (until a stable voltammogram was obtained), cleaned by sonication in ddH_2O, and dried with N_2. For the attachment of PSA peptides, the cleaned AuE was incubated with 10 μL of 1.5 μM PSA peptide at 37 °C for 0.5 h and rinsed thoroughly with ddH_2O. The obtained AuE/P_{PSA} was then backfilled with 2 mM MCH in 60% ethanol at 37 °C for 15 min and rinsed with ethanol and ddH_2O. Further, the obtained AuE/MCH/P_{PSA} was incubated with 10 μL of PSA at 37 °C for 1 h and rinsed thoroughly with the washing buffer; the obtained gold electrode was noted as AuE/MCH/P-COOH. After soaking in 2 mM $ZrOCl_2$ in 20% ethanol at 37 °C for 0.5 h and a rigorous rinse with ddH_2O, the obtained AuE/MCH/P-COOH/Zr(IV) was incubated with 1 mM BPAA in 40% ethanol at 37 °C for 0.5 h, and rinsed with copious ethanol and ddH_2O. For the grafting of ferrocenyl polymers, the obtained AuE/MCH/P-COOH/Zr(IV)/BPAA was soaked in the polymerization solution, followed by the eATRP of FcMMA under potentiostatic conditions for 45 min using an amperometric *i*−*t* curve. After linear sweep voltammetry (LSV) from 0 to 0.2 V several times (to remove the Cu(0) residues[45]), the as-modified AuE/MCH/P-COOH/Zr(IV)/BPAA/Fc was rinsed with copious ethanol and ddH_2O, dried with N_2, and finally examined in 0.5 M $LiClO_4$ by square wave voltammetry (SWV; quiet time, 15 s; potential increase, 4 mV; potential amplitude, 25 mV).[50]

RESULTS AND DISCUSSION

Electrogeneration of the Cu^I/Me_6TREN Activators. In ATRP, the dynamic equilibrium between the active radicals and the dormant species (R−X or P_n−X) is mediated by the activator/deactivator couple.[47] For the Cu-based ATRP system, specifically, the Cu^I/ligand activators react with the dormant species to form the $Cu^{II}X$/ligand deactivators and the active radicals, which can either propagate by reacting with monomers to form polymer chains or revert back to the dormant species by reacting with the $Cu^{II}X$/ligand deactivators.[45] As a result of the dynamic equilibrium, the concentration of the active radicals can be sustained at a very low level, enabling good control over the polymerization process by substantially suppressing the biradical termination.[37] In the eATRP-based method, the Cu^I/Me_6TREN activators were potentiostatically generated by the electrochemical reduction of the $Cu^{II}Br/Me_6TREN$ deactivators. As is evident from the Nernst equation (eq 1, in which $E^{\circ\prime}$, *R*, and *F* represent the apparent formal potential of the [Cu^I/Me_6TREN]/[$Cu^{II}Br/Me_6TREN$] redox couple, the universal gas constant, and the Faraday constant, respectively),[45] the stoichiometric ratio of the Cu^I/Me_6TREN activator to the $Cu^{II}Br/Me_6TREN$ deactivator and as a result, the polymerization rate can be precisely controlled by the applied potential (E_{app}). Through E_{app} biasing, the eATRP can be initiated, ceased, and rejuvenated at will,[48] providing the opportunity to temporally control the polymerization process, which is advantageous to polymer synthesis and surface functionalization.

$$E_{app} = E^{\circ\prime} + \frac{RT}{nF}\ln\frac{C_{[Cu^{II}Br/Me6TREN]}}{C_{[Cu^{I}/Me6TREN]}} \quad (1)$$

To potentiostatically generate the Cu^I/Me_6TREN activators, the typical cyclic voltammogram curves of the AuE/MCH/P-COOH/Zr(IV)/BPAA in the FcMMA-free polymerization solution was acquired. As shown in Figure S1, the cathodic scan resulted in a reduction peak at −0.53 V, corresponding to the electrochemical reduction of the $Cu^{II}Br/Me_6TREN$ deactivators into the Cu^I/Me_6TREN activators.[45] As a more negative E_{app} would result in the generation of a higher amount of Cu^I/Me_6TREN activator, and thus a higher polymerization rate, the subsequent grafting of polymers was carried out at −0.6 V. As is evident from Figure S2, the reduction wave of oxygen overlaps with that of the $Cu^{II}Br/Me_6TREN$ deactivator. That is, the dissolved oxygen is consumed during the electrogeneration of Cu^I/Me_6TREN activators. Such that, the eATRP of FcMMA in this work can be performed without deoxygenating.

Characterization. In this report, the PSA peptide as the specific MRE for PSA was end-attached to the gold surface via the sulfur−gold self-assembly. Through reductive desorption of thiol in 0.5 M KOH (N_2 saturated) by LSV (Figure S3), the coverage (Γ_{real}) of the surface-attached PSA peptide was found to be 1.72×10^{-10} mol cm^{-2}, indicating that ∼81.4% of the pre-added PSA peptides have been attached to the gold surface. For the PSA peptide, the maximal coverage (Γ_{max}) was measured to be 3.56×10^{-10} mol cm^{-2}. That is, about 48.3% of the binding sites for PSA peptide could be actually occupied.

https://dx.doi.org/10.1021/acs.analchem.0c03467
Anal. Chem. XXXX, XXX, XXX−XXX

For the cleavage-based electrochemical PSA biosensor, the target-induced cleavage of PSA peptides generated the carboxyl sites, through which the BPAA initiators for the eATRP of FcMMA were then linked via the Zr(IV) linkers. To evaluate the feasibility of the cleavage-based electrochemical PSA biosensor, the square wave voltammograms of differently modified electrode surfaces were collected (Figure 1A). As

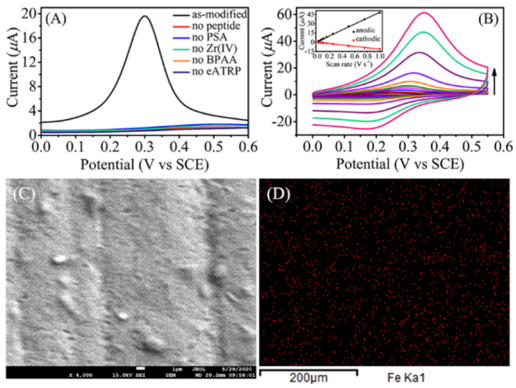

Figure 1. (A) Square wave voltammograms collected from differently modified electrodes. (B) Cyclic voltammograms of the as-modified AuE/MCH/P-COOH/Zr(IV)/BPAA/Fc in 0.5 M $LiClO_4$ at a scan rate ranging from 0.015 to 1.0 V s^{-1}. Inset: Plots of anodic (▲) and cathodic (Red Triangle Down Solid) peak currents versus scan rate. (C) SEM image of the AuE/MCH/P-COOH/Zr(IV)/BPAA/Fc. (D) Elemental mapping of Fe. In these experiments, the concentration of PSA was 10 nM.

observed, the as-modified AuE/MCH/P-COOH/Zr(IV)/BPAA/Fc had a high oxidation peak at 0.3 V, showing the presence of a large amount of Fc redox tags.[45] Furthermore, the redox properties of Fc tags were studied based on the scan rate-dependent cyclic voltammograms (Figure 1B). As the scan rate increased from 0.015 to 1 V s^{-1}, the anodic (▲) and cathodic (Red Triangle Down Solid) peak currents were found to increase linearly (see the inset in Figure 1B). This observation agrees well with the surface-confined redox process.[41,43] To provide solid evidence of the presence of ferrocenyl polymers, the surface features and elemental compositions of AuE/MCH/P-COOH/Zr(IV)/BPAA/Fc were determined by SEM and energy-dispersive X-ray (EDX) spectroscopy, respectively. According to the results shown in Figure 1C,D, it could be concluded that on the electrode surface, there is a densely-packed ferrocenyl polymer layer. In addition, the elemental mappings of Zr and Br, as shown in Figure S4A,B evidenced the presence of the Zr(IV) linkers and the BPAA initiators, respectively.[45] As is evident from Figure 1A, the absence of PSAs would result in a negligible background current. This is expected because, in such a case, there were no carboxyl sites available for the labeling of the BPAA initiators. For the cases without PSA peptides, Zr(IV) linkers, BPAA initiators, or eATRP, similarly, no clear oxidation peak could be observed. Because the oxidation peak could only be observed from the perfectly-modified surface, the cleavage-based electrochemical biosensor is believed to be highly applicable to PSA detection.

The fabrication of the cleavage-based electrochemical PSA biosensor was further confirmed by EIS. Shown in Figure 2A are the Nyquist plots. As a measure of the interfacial charge transfer kinetics, the charge transfer resistance (R_{ct}) can be derived from the equivalent circuit, expressed in the model of

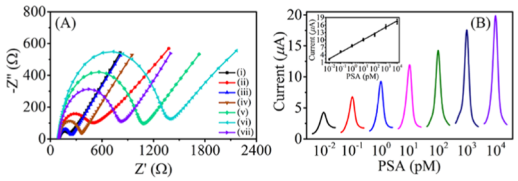

Figure 2. (A) Nyquist plots of (i) the bare AuE, (ii) AuE/P_{PSA}, (iii) AuE/MCH/P_{PSA}, (iv) AuE/MCH/P-COOH, (v) AuE/MCH/P-COOH/Zr(IV), (vi) AuE/MCH/P-COOH/Zr(IV)/BPAA, and (vii) AuE/MCH/P-COOH/Zr(IV)/BPAA/Fc. PSA, 10 nM. (B) Square wave voltammograms derived from different PSA concentrations (from 10 fM to 10 nM). Inset: Calibration plot of peak current versus the logarithm of PSA concentration. Error bars show the standard deviations (n = 4).

$R_s(Q(R_{ct}W))$, where R_s, Q, and W represent the solution resistance, the constant-phase element (CPE), and the Warburg resistance, respectively. The bare AuE was found to show a small R_{ct} (~137 Ω, curve i), which agrees well with the fast charge transfer kinetics.[43] Due to the presence of steric hindrance,[41] the attachment of PSA peptides brought the R_{ct} to ~372 Ω (curve ii). After the backfilling of the peptide monolayer with MCH, the R_{ct} decreased to ~142 Ω (curve iii). Such an observation reveals that the formation of the two-component monolayer of the PSA peptide and MCH favors interfacial charge transfer. This is likely due to the backfilling-induced reconfiguration of the peptide monolayer.[51] Prior to backfilling with MCH, the PSA peptides can interact with the gold surface through both the sulfur atom of the *N*-terminal cysteine residue and the amino groups on the side chains.[52] As a result, a majority of PSA peptides were actually bound to the gold surface through nonspecific adsorption. Due to the presence of the nonspecific interactions, undoubtedly, the surface-bound PSA peptides would be in a flat-lying configuration.[51] The backfilling with an MCH layer would not only result in the removal of the nonspecifically-bound PSA peptides but can also force the specifically-attached ones to rearrange into a standing-up configuration.[52] That is, the backfilling of the peptide monolayer with MCH can largely moderate the steric hindrance, thereby facilitating the charge transfer. After incubation with PSA, the R_{ct} increased to ~252 Ω (curve iv), indicative of the generation of the negatively-charged carboxyl sites, which are adverse to charge transfer.[51] As shown, further incubation with the Zr(IV) linkers (~943 Ω, curve v) and the BPAA initiators (~1.24 kΩ, curve vi) resulted in the increase of the R_{ct}, which are in line with our previous observations.[43,45] After eATRP of FcMMA, the R_{ct} decreased to ~702 Ω (curve vii). This is not surprising because the densely-packed ferrocenyl polymer layer can greatly facilitate the charge transfer.[41] These results demonstrate that the PSA biosensor can be fabricated as expected.

Analytical Performance. The analytical performance of the cleavage-based electrochemical PSA biosensor was evaluated by the quantitative assays. Figure 2B shows the square wave voltammograms corresponding to a concentration range of over 7 orders of magnitude from 10 fM to 10 nM. As seen, the peak current increased with the increase of PSA concentration, indicating that the concentration of PSA can be assayed in a signal-on format, being less sensitive to the false positives. The peak current was observed to correlate linearly with the logarithm of PSA concentration. The regression equation of the calibration plot can be expressed as I_p (μA) = 2.542 × lg[C_{PSA}/pM] + 7.547 (R^2 = 0.996). The LOD was

https://dx.doi.org/10.1021/acs.analchem.0c03467
Anal. Chem. XXXX, XXX, XXX−XXX

Table 1. Comparison of the Analytical Performance of Different Methods for PSA Detection

method	recognition element	signal amplification	dynamic range	LOD	refs
fluorescence	antibody	no	0.6−100 ng mL^{-1}	0.6 ng mL^{-1}	4
colorimetric	antibody	HRP[a]	0.825−165 ng mL^{-1}	0.16 ng mL^{-1}	6
DLS[a]	antibody	no	0−6 pM	0.4 pM	8
RLS[a]	aptamer	no	0.13−110 ng mL^{-1}	32 pg mL^{-1}	9
ECL	peptide substrate	Nafion	0.005−5 ng mL^{-1}	0.8 pg mL^{-1}	10
CL	antibody	soybean peroxidase	0.02−125 ng mL^{-1}	7 pg mL^{-1}	12
PEC	antibody	HCR[a]	0.005−20 ng mL^{-1}	1.5 pg mL^{-1}	17
SERS	aptamer	AuNPs	5−500 pg mL^{-1}	5 pg mL^{-1}	18
electrochemical	antibody	HRP-MWCNTs[a]	0.001−10 ng mL^{-1}	0.4 pg mL^{-1}	28
electrochemical	antibody	Fe_3O_4 NPs	0.01−40 ng mL^{-1}	2 pg mL^{-1}	30
electrochemical	antibody	AuNPs-HRP	0−0.1 ng mL^{-1}	1 pg mL^{-1}	31
electrochemical	peptide substrate	no	0.5−40 ng mL^{-1}	0.2 ng mL^{-1}	33
electrochemical	peptide substrate	GO-Fe_3O_4-Thi[a]	0.005−10 ng mL^{-1}	0.76 pg mL^{-1}	13
electrochemical	peptide substrate	electrocatalysis	not provided	1 pM	34
electrochemical	peptide substrate	eATRP	10 fM−10 nM	3.2 fM (0.109 pg mL^{-1})	this work

[a]HRP, horseradish peroxidase; DLS, dynamic light scattering; RLS, resonance light scattering; HCR, hybridization chain reaction; MWCNTs, multiwall carbon nanotubes; and GO-Fe_3O_4-Thi, graphene oxide-Fe_3O_4-thionine.

calculated based on the $3\sigma_b$/slope criteria to be 3.2 fM (~0.109 pg mL^{-1}), where σ_b represents the standard deviation of the blank sample. Since the LOD is at the femtomolar level, the cleavage-based electrochemical PSA biosensor is highly sensitive. Summarized in Table 1 is the analytical performance of different methods for PSA detection.[53] Evidently, the LOD of this electrochemical PSA biosensor is much lower than that of other methods. Relative to the method using the Fc-tagged peptide as the MRE,[33] as an example, the LOD has been lowered by around 1835-fold (~0.109 pg mL^{-1} versus 0.2 ng mL^{-1}), although at the expense of a relatively longer turnaround time (longer by about 2.25 h), three more steps in operation, and a lower amplitude in the change of the peak current. The significantly improved detection sensitivity can be attributed to the eATRP-based amplification method, through which a large amount of Fc redox tags can be recruited to amplify the detection signal.

Selectivity, Reproducibility, Storage Stability, and Practicability. In this report, a peptide substrate that is specific for the PSA was used as the MRE. The selectivity of the cleavage-based electrochemical PSA biosensor was studied with CEA, AFP, BSA, IgG, Hb, chymo, and tryp at a concentration of 100 nM, which was 10 times that of PSA (10 nM). Shown in Figure 3A are the peak currents derived from these samples. As seen, the incubation of the AuE/MCH/P_{PSA} with 10 nM PSA could result in the generation of a high peak current. Instead, the incubation with 100 nM other samples caused a negligible change in the peak current relative to the blank sample. Besides, the presence of chymo and tryp had little influence on the peak current relative to PSA alone. High selectivity is expected since the incubation of AuE/MCH/P_{PSA} with other samples other than PSA cannot result in the cleavage of the PSA peptide, which was designed for the specific recognition of PSA.[49]

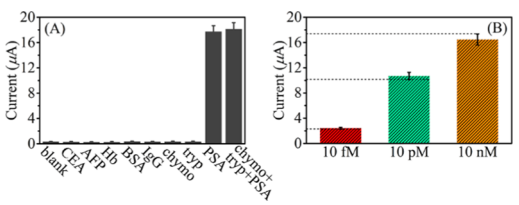

Figure 3. (A) Peak currents derived from different samples and the mixture of chymo, tryp, and PSA (PSA, 10 nM; others, 100 nM). (B) The expected (indicated by black-dashed lines) and the measured peak currents derived from the spiked serum samples. Error bars show standard deviations (n = 4).

The reproducibility of the cleavage-based electrochemical PSA biosensor was evaluated based on the standard deviations of the peak currents derived from the intra-batch and inter-batch experiments, which were performed with two sets of electrodes that were fabricated in the presence of 10 nM PSA. The standard deviation of the intra-batch experiment was 5.3% (n = 4), while for the inter-batch it was 5.8% (n = 4). Thus, the reproducibility of this electrochemical PSA biosensor is satisfactory.

The long-term storage stability of the AuE/MCH/P-COOH/Zr(IV)/BPAA/Fc was tested using eight electrodes, identically fabricated in the presence of 10 nM PSA. Four of them were measured without storage, and the rest were stored at 4 °C. After 2 weeks, the peak current was found to decrease by only 3.2% (Figure S5), indicating the high storage stability of the as-modified electrode.

The practicability of this cleavage-based electrochemical biosensor for the detection of PSA in complex biological samples was studied with normal human serum (NHS) due to the lack of clinical samples from subjects suffering from prostate cancer. Of note, it has been verified that PSA in human serum is enzymatically inactive,[54] due to the complete inhibition by the extracellular serine protease inhibitors α_1-antichymotrypsin (ACT; molecular weight (MW), 68 kDa) and α_2-macroglobulin (MW, 720 kDa), which are present in a 10^4−10^5-fold molar excess compared to PSA in serum.[49] Clearly, it is impossible for any cleavage-based method to detect PSA levels directly in untreated serum samples. To demonstrate this, the cleavage-based electrochemical PSA biosensor was challenged directly with untreated NHS. As expected, little difference was observed for the untreated NHS relative to the blank control (Figure S6). To investigate the anti-interference capability, for this reason, the commercially supplied NHS was filtered using a Millipore Amicon Ultra-15 filter with a cutoff of 30 kDa. As a result, the serum components with a MW higher than 30 kDa, like PSA, ACT,

https://dx.doi.org/10.1021/acs.analchem.0c03467
Anal. Chem. XXXX, XXX, XXX−XXX

α_2-macroglobulin, the PSA−ACT complex, and the PSA−α_2-macroglobulin complex, were removed from the filtered NHS, making it possible to evaluate the anti-interference capability of the cleavage-based methods. The serum samples with the final concentration of PSA at 10 fM, 10 pM, or 10 nM were prepared by spiking appropriate amounts of PSA into the filtered, undiluted NHS. The expected (indicated by black-dashed lines, the values were calculated based on the regression equation of the calibration plot, as shown in Figure 2B), and the measured peak currents are shown in Figure 3B. As observed, the presence of complex serum matrices did not interfere with the peak current. Thus, the anti-interference capability of the cleavage-based electrochemical PSA biosensor is satisfactory; however, it is not suitable for the direct detection of real serum samples (this is a common defect of the cleavage-based methods).

CONCLUSIONS

In summary, we have shown that the cleavage-based electrochemical biosensor is applicable for the highly selective detection of PSA at the femtomolar level, provided that the eATRP-based method is used for signal amplification. Compared with affinity recognition by MIPs, aptamers, or antibodies, the cleavage-based recognition by peptide substrates offers the benefits of improved detection sensitivity and lower detection cost. Through the eATRP-based amplification method, high density of polymers containing a large number of redox tags can be grafted from the electrode surface, generating a sufficiently high detection signal even in the presence of a low-abundance PSA. As a result, the LOD can be pushed down to the femtomolar level. Without the use of enzymes or nanoparticles for signal amplification, the eATRP-based method has the merits of being low-cost and easy to operate. Taking together, the integration of the eATRP-based amplification method into the cleavage-based recognition is applicable to the highly selective and sensitive detection of PSA. In addition, this electrochemical biosensor features satisfactory anti-interference capability for the detection of PSA in complex biological samples and thus holds great promise in clinical applications.

ASSOCIATED CONTENT

Supporting Information

The Supporting Information is available free of charge at https://pubs.acs.org/doi/10.1021/acs.analchem.0c03467.

Electrogeneration of Cu^I/Me_6TREN activators; reduction wave of dissolved oxygen; reductive desorption of the PSA peptide by LSV; elemental mappings of Zr and Br; and storage stability and peak current of the untreated NHS (PDF)

AUTHOR INFORMATION

Corresponding Author

Yuwei Zhang − *Center for Advanced Analytical Science, School of Chemistry and Chemical Engineering, Guangzhou University, Guangzhou 510006, P. R. China;* orcid.org/0000-0002-3040-137X; Phone: +86-020-39366902; Email: ccywzhang@gzhu.edu.cn

Authors

Qiong Hu − *Center for Advanced Analytical Science, School of Chemistry and Chemical Engineering, Guangzhou University, Guangzhou 510006, P. R. China;* orcid.org/0000-0001-6360-1813

Shiyu Gan − *Center for Advanced Analytical Science, School of Chemistry and Chemical Engineering, Guangzhou University, Guangzhou 510006, P. R. China;* orcid.org/0000-0002-5495-4585

Yu Bao − *Center for Advanced Analytical Science, School of Chemistry and Chemical Engineering, Guangzhou University, Guangzhou 510006, P. R. China;* orcid.org/0000-0002-5023-4345

Dongxue Han − *Center for Advanced Analytical Science, School of Chemistry and Chemical Engineering, Guangzhou University, Guangzhou 510006, P. R. China;* orcid.org/0000-0002-7343-2221

Li Niu − *Center for Advanced Analytical Science, School of Chemistry and Chemical Engineering, Guangzhou University, Guangzhou 510006, P. R. China;* orcid.org/0000-0003-3652-2903

Complete contact information is available at: https://pubs.acs.org/10.1021/acs.analchem.0c03467

Author Contributions

All authors have given approval to the final version of the manuscript.

Notes

The authors declare no competing financial interest.

ACKNOWLEDGMENTS

This work was supported by the National Natural Science Foundation of China (21904026), the Project Funded by China Postdoctoral Science Foundation (2018M643040), and the National Natural Science Foundation of China (21974032, 21974031, and 21974033).

REFERENCES

(1) Siegel, R. L.; Miller, K. D.; Jemal, A. *Ca-Cancer J. Clin.* **2020**, *70*, 7−30.

(2) Lewenhaupt, A.; Ekmaim, P.; Eneroth, P.; Nilsson, B. *Br. J. Urol.* **1990**, *66*, 182−187.

(3) Stamey, T. A.; Yang, N.; Hay, A. R.; McNeal, J. E.; Freiha, F. S.; Redwine, E. *N. Engl. J. Med.* **1987**, *317*, 909−916.

(4) Kokko, T.; Liljenbäck, T.; Peltola, M. T.; Kokko, L.; Soukka, T. *Anal. Chem.* **2008**, *80*, 9763−9768.

(5) Liu, D.; Huang, X.; Wang, Z.; Jin, A.; Sun, X.; Zhu, L.; Wang, F.; Ma, Y.; Niu, G.; Walker, A. R. H.; Chen, X. *ACS Nano* **2013**, *7*, 5568−5576.

(6) Lang, Q.; Wang, F.; Yin, L.; Liu, M.; Petrenko, V. A.; Liu, A. *Anal. Chem.* **2014**, *86*, 2767−2774.

(7) Shao, F.; Zhang, L.; Jiao, L.; Wang, X.; Miao, L.; Li, H.; Zhou, F. *Anal. Chem.* **2018**, *90*, 8673−8679.

(8) Liu, X.; Dai, Q.; Austin, L.; Coutts, J.; Knowles, G.; Zou, J.; Chen, H.; Huo, Q. *J. Am. Chem. Soc.* **2008**, *130*, 2780−2782.

(9) Chen, Z.; Lei, Y.; Chen, X.; Wang, Z.; Liu, J. *Biosens. Bioelectron.* **2012**, *36*, 35−40.

(10) Qi, H.; Li, M.; Dong, M.; Ruan, S.; Gao, Q.; Zhang, C. *Anal. Chem.* **2014**, *86*, 1372−1379.

(11) Zhang, J.; Qi, H.; Li, Z.; Zhang, N.; Gao, Q.; Zhang, C. *Anal. Chem.* **2015**, *87*, 6510−6515.

(12) Liu, A.; Zhao, F.; Zhao, Y.; Shangguan, L.; Liu, S. *Biosens. Bioelectron.* **2016**, *81*, 97−102.

(13) Huang, Y.; Wang, T. H.; Jiang, J. H.; Shen, G. L.; Yu, R. Q. *Clin. Chem.* **2009**, *55*, 964−971.

(14) Briman, M.; Artukovic, E.; Zhang, L.; Chia, D.; Goodglick, L.; Gruner, G. *Small* **2007**, *3*, 758−762.

(15) Zhang, K.; Lv, S.; Lin, Z.; Li, M.; Tang, D. *Biosens. Bioelectron.* **2018**, *101*, 159−166.
(16) Zhao, W. W.; Dong, X. Y.; Wang, J.; Kong, F. Y.; Xu, J. J.; Chen, H. Y. *Chem. Commun.* **2012**, *48*, 5253−5255.
(17) Zhao, J.; Wang, S.; Zhang, S.; Zhao, P.; Wang, J.; Yan, M.; Ge, S.; Yu, J. *Biosens. Bioelectron.* **2020**, *150*, No. 111958.
(18) Yang, K.; Hu, Y.; Dong, N.; Zhu, G.; Zhu, T.; Jiang, N. *Biosens. Bioelectron.* **2017**, *94*, 286−291.
(19) Grubisha, D. S.; Lipert, R. J.; Park, H. Y.; Driskell, J.; Porter, M. D. *Anal. Chem.* **2003**, *75*, 5936−5943.
(20) Ding, Y.; Lu, H.; Shi, G.; Liu, J.; Shen, G.; Yu, R. *Biosens. Bioelectron.* **2008**, *24*, 228−232.
(21) Saerens, D.; Frederix, F.; Reekmans, G.; Conrath, K.; Jans, K.; Brys, L.; Huang, L.; Bosmans, E.; Maes, G.; Borghs, G.; Muyldermans, S. *Anal. Chem.* **2005**, *77*, 7547−7555.
(22) Das, J.; Aziz, M. A.; Yang, H. *J. Am. Chem. Soc.* **2006**, *128*, 16022−16023.
(23) Strzemińska, I.; Fanchine, S. S. R.; Anquetin, G.; Reisberg, S.; Noël, V.; Pham, M. C.; Piro, B. *Biosens. Bioelectron.* **2016**, *81*, 131−137.
(24) Zhang, J.; Ting, B. P.; Khan, M.; Pearce, M. C.; Yang, Y.; Gao, Z.; Ying, J. Y. *Biosens. Bioelectron.* **2010**, *26*, 418−423.
(25) Wei, Q.; Zhao, Y.; Xu, C.; Wu, D.; Cai, Y.; He, J.; Li, H.; Du, B.; Yang, M. *Biosens. Bioelectron.* **2011**, *26*, 3714−3718.
(26) Patra, S.; Roy, E.; Madhuri, R.; Sharma, P. K. *Biosens. Bioelectron.* **2015**, *66*, 1−10.
(27) Souada, M.; Piro, B.; Reisberg, S.; Anquetin, G.; Noël, V.; Pham, M. C. *Biosens. Bioelectron.* **2015**, *68*, 49−54.
(28) Akter, R.; Rahman, M. A.; Rhee, C. K. *Anal. Chem.* **2012**, *84*, 6407−6415.
(29) Pampalakis, G.; Kelley, S. O. *Analyst* **2009**, *134*, 447−449.
(30) Li, H.; Wei, Q.; He, J.; Li, T.; Zhao, Y.; Cai, Y.; Du, B.; Qian, Z.; Yang, M. *Biosens. Bioelectron.* **2011**, *26*, 3590−3595.
(31) Chen, X.; Zhou, G.; Song, P.; Wang, J.; Gao, J.; Lu, J.; Fan, C.; Zuo, X. *Anal. Chem.* **2014**, *86*, 7337−7342.
(32) Chuah, K.; Lai, L. M.; Goon, I. Y.; Parker, S. G.; Amal, R.; Gooding, J. J. *Chem. Commun.* **2012**, *48*, 3503−3505.
(33) Zhao, N.; He, Y.; Mao, X.; Sun, Y.; Zhang, X.; Li, C. Z.; Lin, Y.; Liu, G. *Electrochem. Commun.* **2010**, *12*, 471−474.
(34) Roberts, M. A.; Kelley, S. O. *J. Am. Chem. Soc.* **2007**, *129*, 11356−11357.
(35) He, Y.; Xie, S.; Yang, X.; Yuan, R.; Chai, Y. *ACS Appl. Mater. Interfaces* **2015**, *7*, 13360−13366.
(36) Lou, X.; Lewis, M. S.; Gorman, C. B.; He, L. *Anal. Chem.* **2005**, *77*, 4698−4705.
(37) Hu, Q.; Gan, S.; Bao, Y.; Zhang, Y.; Han, D.; Niu, L. *J. Mater. Chem. B* **2020**, *8*, 3327−3340.
(38) Yuan, L.; Wei, W.; Liu, S. *Biosens. Bioelectron.* **2012**, *38*, 79−85.
(39) Wu, Y.; Wei, W.; Liu, S. *Acc. Chem. Res.* **2012**, *45*, 1441−1450.
(40) Wu, Y.; Liu, S.; He, L. *Anal. Chem.* **2009**, *81*, 7015−7021.
(41) Hu, Q.; Bao, Y.; Gan, S.; Zhang, Y.; Han, D.; Niu, L. *Biosens. Bioelectron.* **2020**, *165*, No. 112358.
(42) Qian, H.; He, L. *Anal. Chem.* **2009**, *81*, 9824−9827.
(43) Hu, Q.; Wang, Q.; Jiang, C.; Zhang, J.; Kong, J.; Zhang, X. *Biosens. Bioelectron.* **2018**, *110*, 52−57.
(44) Qian, H.; He, L. *Anal. Chem.* **2009**, *81*, 4536−4542.
(45) Hu, Q.; Wang, Q.; Sun, G.; Kong, J.; Zhang, X. *Anal. Chem.* **2017**, *89*, 9253−9259.
(46) Hu, Q.; Wang, Q.; Kong, J.; Li, L.; Zhang, X. *Biosens. Bioelectron.* **2018**, *101*, 1−6.
(47) Wang, J. S.; Matyjaszewski, K. *J. Am. Chem. Soc.* **1995**, *117*, 5614−5615.
(48) Magenau, A. J.; Strandwitz, N. C.; Gennaro, A.; Matyjaszewski, K. *Science* **2011**, *332*, 81−84.
(49) Denmeade, S. R.; Lou, W.; Lövgren, J.; Malm, J.; Lilja, H.; Isaacs, J. T. *Cancer Res.* **1997**, *57*, 4924−4930.
(50) Hu, Q.; Kong, J.; Han, D.; Bao, Y.; Zhang, X.; Zhang, Y.; Niu, L. *Talanta* **2020**, *206*, No. 120173.
(51) Hu, Q.; Bao, Y.; Gan, S.; Zhang, Y.; Han, D.; Niu, L. *Anal. Chem.* **2020**, *92*, 3470−3476.
(52) Herne, T. M.; Tarlov, M. J. *J. Am. Chem. Soc.* **1997**, *119*, 8916−8920.
(53) Ding, C.; Wang, X.; Luo, X. *Anal. Chem.* **2019**, *91*, 15846−15852.
(54) Mikolajczyk, S. D.; Marks, L. S.; Partin, A. W.; Rittenhouse, H. G. *Urology* **2002**, *59*, 797−802.

https://dx.doi.org/10.1021/acs.analchem.0c03467
Anal. Chem. XXXX, XXX, XXX−XXX